Exciton Annihilation and Energy Transfer in Self-Assembled Peptide-Porphyrin Complexes Depends on Peptide Secondary Structure

ARTICLE *in* THE JOURNAL OF PHYSICAL CHEMISTRY B · NOVEMBER 2010

Impact Factor: 3.3 · DOI: 10.1021/jp108685n · Source: PubMed

Exciton Annihilation and Energy Transfer in Self-Assembled Peptide−Porphyrin Complexes Depends on Peptide Secondary Structure

Darius Kuciauskas,[§,*,†] Juris Kiskis,[‡] Gregory A. Caputo,[*,†] and Vidmantas Gulbinas[*,‡]

Department of Chemistry and Biochemistry, Rowan University, 201 Mullica Hill Road, Glassboro, New Jersey 08108, United States and Institute of Physics, Centre for Physical and Technological Sciences, Savanoriu 238, Vilnius, Lithuania

Received: September 12, 2010; Revised Manuscript Received: October 19, 2010

We used picosecond transient absorption and fluorescence lifetime spectroscopy to study singlet exciton annihilation and depolarization in self-assembled aggregates of *meso*-tetra(4-sulfonatophenyl)porphine ($TPPS_4$) and a synthetic 22-residue polypeptide. The polypeptide was designed and previously shown to bind three $TPPS_4$ monomers via electrostatic interactions between the sulfonate groups and cationic lysine residues. Additionally, the peptide induces formation of $TPPS_4$ J-aggregates in acidic solutions when the peptide secondary structure is disordered. In neutral solutions, the peptide adopts an α-helical secondary structure that can bind $TPPS_4$ with high affinity but J-aggregate formation is inhibited. Detailed analysis of excitation-power dependent transient absorption kinetics was used to obtain rate constants describing the energy transfer between $TPPS_4$ molecules in an aggregate under acidic and neutral conditions. Independently, such analysis was confirmed by picosecond fluorescence emission depolarization measurements. We find that energy transfer between $TPPS_4$ monomers in a peptide−$TPPS_4$ complex is more than 30 times faster in acidic aqueous solution than in neutral solutions (9 vs 279 ps). This result was attributed to a conformational change of the peptide backbone from disordered at low pH to α-helical at neutral pH and suggests a new approach to control intermolecular energy transfer with possible applications in fluorescent sensors or biomimetic light harvesting antennas.

Introduction

The absorption of solar energy and conversion into usable chemical energy is a common theme found in plants and photosynthetic bacteria. This absorption and conversion employs a variety of specialized, membrane-bound components that serve as absorbing antennas and reaction centers.[1] The light-harvesting antennas are evolutionarily optimized for efficient absorption of solar radiation as well as excited state energy transfer to photochemical reaction centers. Such antennas consist of several to several hundred light absorbing chromophores arranged in well-defined structures. Excitonic interactions between the light-absorbing chromophores lead to red shifts in the absorption spectra and efficient energy transfer between the antenna components.[1] Mimicry of photosynthetic antenna structures is potentially useful for third-generation photovoltaics and can potentially aid in understanding these complex biological systems.[2]

Numerous peptides and proteins designed to bind porphyrins have been successfully synthesized and characterized. The peptide−porphyrin binding in these proteins is mediated either through amino acid side chains chelating a metal ion at the center of the porphyrin or through amino acid interactions with the porphyrin side chains. The metal-chelating constructs typically are designed such that specific amino acid side chains favorably interact with the metal ion, similar to the histidine-based chelation of iron in hemoglobin.[3−10] Many of these constructs are based on the biologically relevant four-helix bundle motif, which allows positioning of the porphyrin at the helical interface. The alternative design is one in which the porphyrin is bound through side-chain interactions. These designs use smaller, synthetic peptides that lack significant tertiary and quartenary structure, unlike the 4-helix bundles.[11−13]

Recently we designed and characterized self-assembled light-harvesting antennas consisting of a 22-residue peptide and three anionic *meso*-tetra(4-sulfonatophenyl)porphine ($TPPS_4$) monomers (Scheme 1).[15] The cationic lysine side chains were used to bind sulfonate groups of $TPPS_4$ via electrostatic interactions. Using absorption, fluorescence, resonant light scattering (RLS), and circular dichroism (CD) spectroscopy, we have shown that one peptide with nine lysine residues binds three porphyrin monomers (i.e., 3 lysine residues per $TPPS_4$ molecule). In acidic solutions (pH 1.8 and 3.6) where the peptide has disordered secondary structure, peptide-bound porphyrins were shown to form J-aggregates. In neutral solutions (pH 7.6), porphyrin binding to the peptide induces α-helical secondary structure for a portion of the peptide. However, $TPPS_4$ J-aggregates are not formed at neutral pH. The interplay between peptide secondary structure and the ability of $TPPS_4$ (or other porphyrins) to form excitonically coupled J-aggregates could be useful for the rational design of new peptide−porphyrin based antennas.

Only dynamic studies with sufficient (fs/ps) time resolution could directly examine energy transfer in such self-assembled aggregates. This system poses an additional complication in that all porphyrins are assumed to be equivalent. Therefore, monitoring time-dependent spectral changes to reveal energy transfer pathways is not possible. In light of this, we used ultrafast nonlinear spectroscopy based on singlet exciton annihilation.

* To whom correspondence should be addressed. E-mail: (D.K.) Darius.Kuciauskas@nrel.gov; (G.A.C.) caputo@rowan.edu; (V.G.) vidgulb@ktl.mii.lt.

† Rowan University.

‡ Centre for Physical and Technological Sciences.

§ Current address: National Renewable Energy Laboratory, 1617 Cole Blvd, Golden, CO 80401.

10.1021/jp108685n
Published on Web 11/11/2010

SCHEME 1: Peptide Sequence, Porphyrin Structure, and an Illustration of a Potential Aggregate Structure in Neutral and Acidic Solutions[14] [a]

KKLIKVWAKGFKKAKKLFKGIG-$CONH_2$

PBR1 PBR2 PBR3

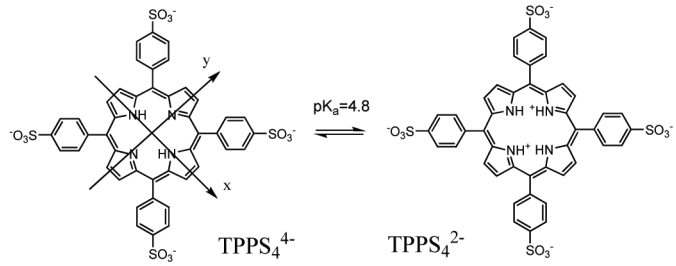

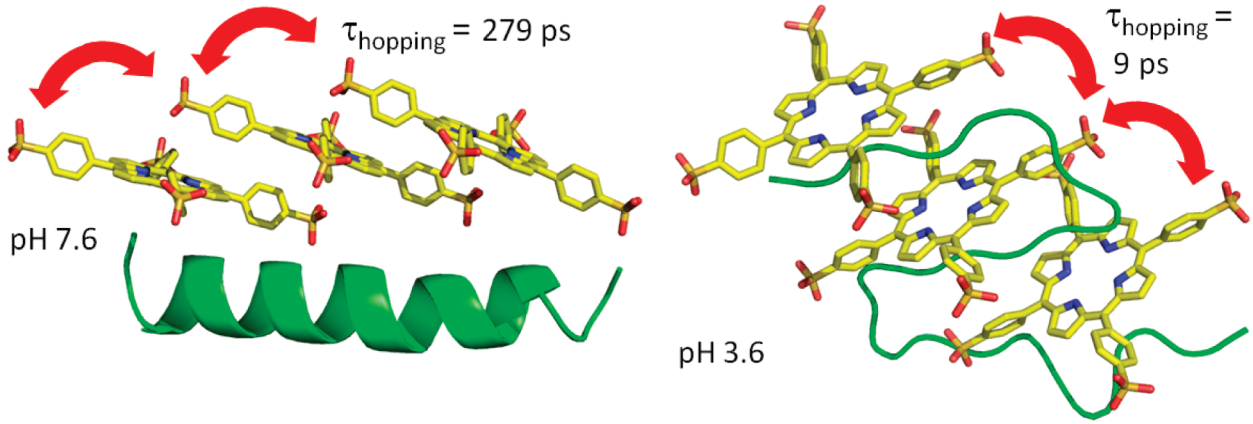

[a] Single-letter abbreviations are used for amino acids. K (shown in blue) is lysine. PBR1-3 are porphyrin binding regions of the polypeptide sequence.

The time-dependence of exciton annihilation (i.e., the disappearance of some excitations after an ultrafast laser pulse at $t = 0$ ps) is dependent on the geometry of the system, orientation, and distance between the transition dipole moments and thus provides a very useful approach to characterize energy transfer in such aggregates. In addition, we investigated fluorescence emission depolarization using time-correlated single photon counting. Both ultrafast spectroscopic techniques yielded consistent picture of energy transfer in self-assembled peptide−porphyrin aggregates.

Materials and Methods

Peptide−Porphyrin Complexes. The structure of *meso*-tetra(4-sulfonatophenyl)porphine ($TPPS_4$, purchased from Frontier Scientific) and the amino acid sequence of the 22-residue peptide are shown in Scheme 1. The peptide contains three groups of cationic lysine (K) residues located at the (i, $i + 1$, $i + 4$) or (i, $i + 3$, $i + 4$, which is the identical arrangement but with opposite directionality) positions in the peptide backbone. The peptide design was based on naturally occurring antimicrobial peptides that are known to undergo helix−coil transitions driven by binding to bacterial cell surfaces or lipid membranes.[16,17] Earlier results showed that three $TPPS_4$ monomers bind to one peptide, which suggests that each (i, $i + 1$, $i + 4$) lysine residue group, or porphyrin binding region (PBR1−PBR3, Scheme 1), binds three sulfonate groups of $TPPS_4$.[15] $TPPS_4$ binding to three lysine residues was also demonstrated for a different peptide sequence.[12,13]

Ten millimolar TRIS·HCl buffer was used for the studies at pH 7.6, while 10 mM citrate buffer was used at pH 3.6.

TABLE 1: Peptide−$TPPS_4$ Complexes Used in Transient Absorption Studies

sample	pH	[peptide], μM	[$TPPS_4$], μM	[peptide]−[$TPPS_4$]	[lysine]−[$TPPS_4$]
B1	3.6	9	9	1:1	9:1
B2	3.6	3	9	1:3	3:1
B3	7.6	3	9	1:3	3:1

Peptide−porphyrin binding stoichiometry (Table 1) was established from previous experiments.[15] The samples described in Table 1 are named **B1**−**B3** for ease of reference.

Spectroscopy. Absorption spectra were measured with a Perkin-Elmer Lambda 35 spectrometer. Fluorescence emission spectra were measured with a Jobin Yvon Fluoromax-2 spectrofluorometer as previously described.[15] Fluorescence emission kinetics were measured using time-correlated single photon counting (TCSPC) with a F900 spectrometer (Edinburgh Instruments). A pulsed diode laser EPL-375 (50 ps pulses at 375 nm with 0.15 mW average power and 20 MHz repetition rate) was used for excitation. After deconvolution, the time resolution of TCSPC setup was about 100 ps. Ten millimeter optical path length quartz cuvettes were used in fluorescence studies.

Transient absorption (TA) was investigated using femtosecond pump−probe spectroscopy. The spectrometer was based on an amplified Ti:Sapphire laser (Integra-C, Quantronix, 130 fs pulses at 805 nm and 1 kHz repetition rate). An optical parametric amplifier (TOPAS C, Light Conversion) was used to obtain excitation pulses. White light continuum generated in a 2 mm thick sapphire plate was used to probe the transient absorption. One millimeter and 2 mm optical path length cuvettes were used in TA studies. The polarization of the pump

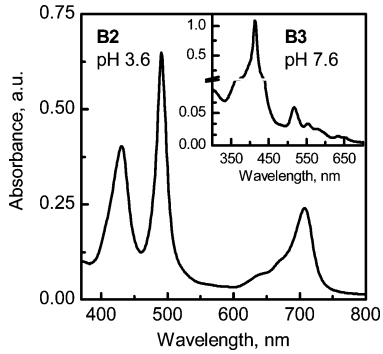

Figure 1. Absorption spectra of peptide−porphyrin aggregates **B2** (pH 3.6) and **B3** (pH 7.6, inset).

and probe pulses were set with Glan laser polarizers. For measuring annihilation kinetics, polarization of the pump and probe pulses were set at the magic angle (54.7°). For TA anisotropy studies, the polarization of the pump and probe pulses was either collinear (signal $I_{//}$) or perpendicular ($I_{\perp}$). The anisotropy values, r, were calculated as

$$r = \frac{I_{II} - I_{\perp}}{I_{II} + 2I_{\perp}} \quad (1)$$

Results and Discussion

Absorption Spectra. Absorption spectra for peptide−$TPPS_4$ complexes are shown in Figure 1. As shown in the inset, at pH 7.6 the Soret band (corresponding to S_2 state of a porphyrin) exhibits maximum absorbance at 413 nm, while several vibronic transitions attributed to the S_1 state are observed at 517 nm (Q_y 0-1 vibronic transition), 554 nm (Q_y 0-0 vibronic transition), ~583 nm (Q_x 0-1 vibronic transition), and ~635 nm (Q_x 0-0 vibronic transition). This spectrum is similar to that of $TPPS_4$ monomer at the same pH, except some changes in absorption band intensity and small spectral shifts, which is indicative of porphyrins binding to peptides.[15] At pH 3.6, when the protonated porphine core has D_{4h} symmetry (Scheme 1), binding to the peptide leads to $TPPS_4$ J-aggregate formation, likely due to electrostatic interactions between the negatively charged sulfonate groups and positively charged pyrolles of porphine macrocycle.[18] Such aggregation is not observed at this pH without peptides present in solution and therefore electrostatic interactions of $TPPS_4$ sulfonate groups with cationic lysine residues are also essential for $TPPS_4$ aggregation at pH 3.6.[12,13,15] The peptide−$TPPS_4$ J-aggregates exhibit new absorption bands at 490 nm (Soret, S_2) and 707 nm (Q, S_1).

Fluorescence Emission Spectra and Kinetics. To gain greater insight into the assembly and excited state interactions of the $TPPS_4$ molecules when bound to the peptide, a series of fluorescence experiments were performed. At pH 3.6, $TPPS_4$ monomers exhibit emission maximum at 670 nm (inset in Figure 2a) and fluorescence emission kinetics are single-exponential with a 4.05 ± 0.01 ns lifetime (data not shown). In contrast, when $TPPS_4$ is bound to peptides at pH 3.6, the $TPPS_4$ fluorescence emission spectrum shows two maxima at 670 and 718 nm, and the fluorescence emission quantum yield is much lower. The 718 nm peak is attributed to $TPPS_4$ J-aggregate emission.[15] Deconvolution of 720 nm emission kinetics shown in Figure 2a yielded a biexponential decay with $\tau_1 = 115$ ps (80% amplitude) and $\tau_2 = 3.55$ ns (20% amplitude). The lifetime of the first component approaches the time resolution of the TCSPC spectrometer and a more accurate estimate of the excited state lifetime for $TPPS_4$ J-aggregates was obtained from transient absorption (next section). However, TCSPC kinetics clearly show that J-aggregate emission at 720 nm is quenched on the picosecond time scale. The $\tau_2 = 3.5$ ns component could be attributed to emission of porphyrins that are not excitonically coupled (either $TPPS_4$ in solution or complexes containing only one porphyrin molecule). The fluorescence emission at 670 nm with $\tau = 3.5 \pm 0.1$ ns can also be attributed to monomers (likely in the peptide-bound conformation).

The $TPPS_4$ fluorescence emission lifetimes in the peptide−porphyrin complexes are similar to lifetimes reported for larger $TPPS_4$ J-aggregates.[19,20] For example, $TPPS_4$ J-aggregates in an aqueous solution of 0.02 M HCl exhibited biexponential kinetics (350 ps (36%) and 3.8 ns (64%) lifetimes measured at 710 nm), while kinetics at 670 nm were single exponential with 3.8 ns lifetime.[19] A similar fluorescence emission lifetime (~0.1 ns) was reported for $TPPS_4$ J-aggregates in CTAB solutions.[20]

The origin of $TPPS_4$ J-aggregate picosecond excited-state quenching is still unclear. There is some evidence that it can be attributed to diffusion-controlled exciton quenching by unidentified quenching centers.[21] In that study of larger $TPPS_4$ aggregates, we estimated that the exciton is transferred between about 20 $TPPS_4$ molecules during its lifetime. Such diffusion-limited quenching by a trap within a peptide−porphyrin complex is less likely because of the small size of the aggregate. Similar fast exciton quenching effects were observed in some photosynthetic complexes and remain a subject of investigation.[22]

In contrast, as shown in Figure 2b, $TPPS_4$ fluorescent states are not quenched at neutral pH. Two emission peaks at 645 and 704 nm are attributed to emission from 0-0 and 0-1 vibronic bands of the S_1 state.[15] For $TPPS_4$ monomers in solution at pH 7.6, fluorescence emission kinetics at 645 nm are best fit with 5.7 ns lifetime. For peptide−porphyrin complexes, fluorescence emission kinetics at 645 and 705 nm have the dominant 7.1−8.9 ns component (about 90% of the amplitude). Similar results have been reported. $TPPS_4$ monomer emission at 680 nm had a 9.26 ns lifetime[20] and emission at 650 nm had 9.8 ns lifetime.[23] $TPPS_4$ has higher fluorescence emission yield at neutral pH, which is also consistent with the absence of quenching.[15,20,23]

Taken together, the TCSPC results are in excellent agreement with earlier-reported steady-state fluorescence emission data;[15] in acidic solutions, $TPPS_4$ excited states are quenched on picosecond time scale, while in neutral solutions excited states have much longer lifetimes. Different interactions with the polypeptide at acidic and neutral pH, including changes in the peptide secondary structure, are the likely cause of changes in the excited state dynamics. In the absence of clear excited state energy traps in the system (when all $TPPS_4$ monomers are presumed to be equivalent), singlet−singlet exciton annihilation and depolarization measurements were used to probe energy transfer.

Transient Absorption Kinetics for Peptide−$TPPS_4$ J-Aggregates at pH 3.6. The peptide-induced effects on excited state dynamics were further analyzed using TA spectroscopy, which allowed us to investigate faster time-scale processes and nonemissive states. Samples **B1** and **B2** were excited to the J-aggregate absorption band at 710 nm and probed at 490 nm, the wavelength corresponding to the bleaching of the aggregate's Soret band and maximal transient absorption signal. As summarized in Table 2, bleaching amplitude ΔOD at $t = 0$ ps is approximately proportional to excitation intensity, which shows that TA signal at 490 nm is proportional to the number of excitations (excitons) in the system.

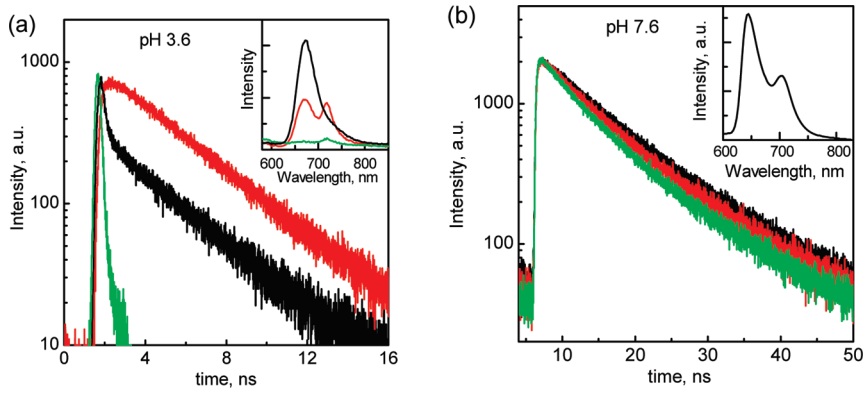

Figure 2. Fluorescence emission kinetics and spectra at pH 3.6 (a) and 7.6 (b). (a) The three emission decays represent the instrumental response function (green line) and 0.4 μM−1.2 μM concentration peptide−$TPPS_4$ samples measured at 670 nm (red line) and 720 nm (black line). Inset in (a) shows emission spectra when $TPPS_4$ concentration was 3.75 μM and peptide concentration has increased from 0 μM (black line), 0.4 μM (red line), and 1.2 μM (green line). (b) Kinetics for 1.2 μM−0.4 μM peptide−$TPPS_4$ samples measured at 645 nm (black line) and 705 nm (red line). For comparison, 645 nm kinetics for $TPPS_4$ aqueous solution is also shown (green line). Inset in (b) shows emission spectrum for 0.4 μM−1.2 μM peptide−$TPPS_4$ sample.

TABLE 2: Transient Absorption Decay Parameters for Aggregates B1 and B2 (pH 3.6)[a]

			amplitudes of decay components[c]			
sample[b]	excitation intensity, mJ cm^{-2}	ΔOD × 10^3 at t = 0 ps	τ_1 = 0.3 ps	τ_2 = 3 ps	τ_3 = 65 ps	τ_4 > 1000 ps
B2[d]	0.20	2.22	0%	3.7%	52.2%	44.1%
	0.98	10.9	14.0%	29.9%	26.6%	29.5%
	8.56	54.3	29.1%	33.8%	19.3%	17.8%
B2[e]	8.56	95.3	37.8%	29.7%	15.7%	16.8%
B2[f]	8.56	31.8	28.9%	30.8%	21.4%	18.9%
B1[d]	8.56	39.7	25.1%	29.2%	26.0%	19.7%

[a] Pump and probe wavelengths 710 and 490 nm, respectively. [b] Concentrations are given in Table 1. [c] Using the multiexponential fit $\Delta OD = A_1 \exp(-t/\tau_1) + A_2 \exp(-t/\tau_2) + A_3 \exp(-t/\tau_3) + A_4 \exp(-t/\tau_4)$, where ΔOD is transient absorption amplitude, A_i is fit component amplitude normalized as $A_i/(A_1 + A_2 + A_3 + A_4) \times 100\%$, and τ_i is a lifetime. [d] Polarization between pump and probe beams set at magic angle. [e] Collinear polarization. [f] Perpendicular polarization.

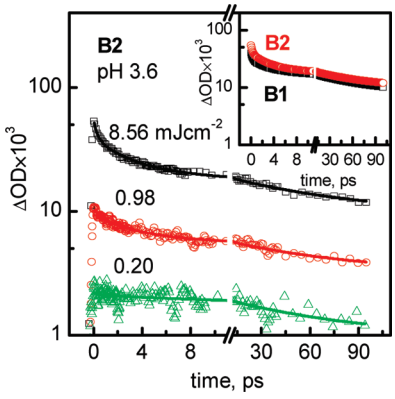

Figure 3. TA kinetics for aggregates **B2** at pH 3.6. Measured at 490 nm with 710 nm excitation, excitation intensity is indicated in the figure. Solid lines represent multiexponential fitting results summarized in Table 2. Inset: Comparison of TA kinetics for **B1** (black) and **B2** (red) measured with 8.56 mJ cm^{-2} excitation. The close similarity of the data supports a cooperative binding model for peptide−porphyrin complexes.

All TA kinetics can be fitted with a sum of four exponential decays with the same time constants of 0.3 ps, 3 ps, 65 ps, and >1 ns (Figure 3 and Table 2). The relative amplitudes of exponential components depend on the excitation intensity that leads to changes in the overall shape of the decay. The lifetimes of slower components, 65 ps and >1 ns, are similar to lifetimes obtained in TCSPC experiments (Figure 2a), thus τ_3 and τ_4 can be attributed to the relaxation of the $TPPS_4$ first excited singlet state. On the basis of their intensity dependence, the two fast components, 0.3 and 3 ps, can be unambiguously attributed to the singlet exciton−exciton annihilation, as explained below. Similar intensity-dependent relaxation in large $TPPS_4$ aggregates has also been attributed to the exciton annihilation.[21] Annihilation studies have been used to analyze energy transfer for small aggregates of three self-assembled porphyrin dimers.[24,25]

Before analyzing the results, we will briefly discuss the annihilation model. When multiple excitations are present in an aggregate, energy transfer from one excited monomer to a second excited monomer becomes possible. When this occurs, the doubly excited state quickly relaxes to its first excited state with excess energy dissipated via vibrational relaxation. As this process depends on the number of excitations in the system, distance between the excited monomers, spectral overlap, and other factors, it provides an important approach to characterize energy transfer in a wide range of molecular systems.[26] The concept of annihilation could become problematic in the case of small J-aggregates, such as trimers, having physical dimensions comparable with the exciton delocalization length. If excitons are delocalized over the entire aggregate, exciton dynamics shall be characterized by the coherent exciton motion rather than exciton hops between individual molecules. At high excitation intensities, when more than one excitation per aggregate is created, the exciton relaxation would be more correctly described by the relaxation of two-exciton or three-exciton states,[27] rather than by the exciton−exciton annihilation. On the other hand, the $TPPS_4$ aggregates are not typical J-aggregates,[28] because strong excitonic coupling is evident only for the Soret band, while excitonic coupling of the lowest excited singlet state forming Q-band, which is responsible for fluorescence, is weaker. Even in large $TPPS_4$ aggregates exciton

delocalization extends over two molecules at most.[21] Therefore the exciton−exciton annihilation model seems to be appropriate in this case where we analyze dynamics of the lowest excited states.

Annihilation is caused by the interaction of several excitons within a single complex, therefore it starts at the intensity at which two excitons are created in one complex. The annihilation in complexes with two excitations (excitons) will result in a fast exponential decay. We attribute the 3 ps decay component to annihilation of two excitons created per complex. At higher excitation intensities, when three excitations per complex are created, the annihilation becomes correspondingly faster and we can attribute a 0.3 ps relaxation component to a three exciton annihilation. Overall, the decay profiles of excited peptide−porphyrin complexes can be described as a sum of three decay processes: exciton−exciton annihilation with decay time τ_1 (three excited porphyrins per complex), exciton−exciton annihilation with decay time τ_2 (two excited porphyrins per complex), and biexponential relaxation of excited state (one excited porphyrin per complex) with decay times τ_3 and τ_4.

Exciton annihilation kinetics also allowed us to independently confirm that peptide−porphyrin binding is cooperative.[15] Inset in Figure 3 compares TA kinetics in samples **B1** and **B2** measured at the same excitation intensity. Both sample compositions have the same $TPPS_4$ concentration, but differ in peptide concentration and hence peptide−$TPPS_4$ ratio (Table 1). The **B2** sample has, on average, three porphyrins per peptide, while for sample **B1** there is only one porphyrin per peptide. The relaxation kinetics for **B1** and **B2**, including exciton annihilation, are surprisingly similar (fitting results are summarized in Table 2). Hence, the data suggest that similar aggregates of three porphyrins and one peptide are formed in both samples, which is in agreement with the cooperative binding model.[15] If binding were not cooperative, much smaller contribution from the fast annihilation decay components would be expected for sample **B1** than for sample **B2**. Simply stated, the cooperative binding model implies that the binding of one ligand will impact the binding energy/affinity of subsequent ligands. This phenomenon was clearly described for the binding of O_2 to the hemoglobin tetramer.[29] When applied to peptide−$TPPS_4$ aggregates, cooperative binding means that the binding constant for the second $TPPS_4$ monomer is larger than that for the first monomer and the binding constant for the third monomer is even greater. Therefore, the solution is predominantly composed of aggregates consisting of one peptide and three porphyrins (and, in the case of **B1**, free peptides). Because TA measures porphyrin spectroscopic properties and $TPPS_4$ aggregates are very similar in samples **B1** and **B2**, TA kinetics in the inset of Figure 3 are comparable.

Transient Absorption Anisotropy Kinetics for Peptide−$TPPS_4$ J-Aggregates at pH 3.6. TA anisotropy (TAA) experiments can provide information about the orientation of the transition dipole moments in complex molecular assemblies. TAA kinetics for sample **B2** are shown in Figure 4, fitting results are given in Table 2. Excitation and probe wavelengths were the same as in experiments described in the previous section. The amplitude of the TA signal measured with collinear polarization of pump and probe beams is ~3 times larger than the amplitude of TA signal measured with perpendicular polarization. According to eq 1, this ratio yields $r \approx 0.4$, which is equal to the maximal possible photoinduced anisotropy for randomly oriented systems.[30]

The inset in Figure 4 shows anisotropy (r) kinetics calculated according to eq 1. Excluding the possible coherent artifacts at

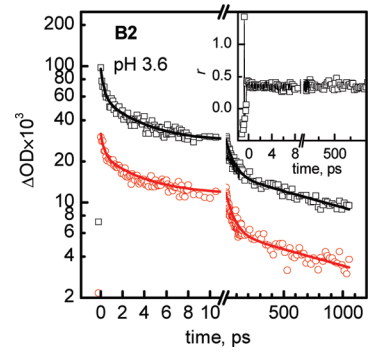

Figure 4. TA kinetics for samples **B2** when polarization of pump and probe beams are collinear (black squares) and perpendicular (red circles). Solid lines represent multiexponential fitting results summarized in Table 2. Inset shows TA anisotropy r values calculated using eq 1. Pump beam wavelength was 710 nm, excitation intensity 8.56 mJ/cm^2, and kinetics were measured at 490 nm.

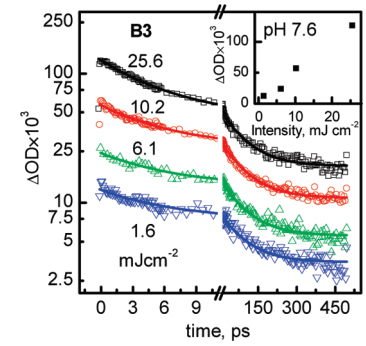

Figure 5. TA kinetics for aggregates **B3** measured at 400 nm with 520 nm excitation, excitation intensity is indicated in the figure. Solid lines represent multiexponential fitting results summarized in Table 3. Inset shows that initial bleaching ΔOD at $t = 0$ ps linearly increases with excitation intensity ($\Delta OD_{t=0\ ps} \propto$ intensity$^{0.97\pm0.11}$).

$t \approx 0$ ps, r has constant amplitude at 0.5 ps < t < 1000 ps and does not show any depolarization. The high anisotropy value indicates that (i) excitonically coupled aggregates may be characterized by the linear transition dipole moment, (ii) the energy transfer between aggregates is absent, and (iii) rotational diffusion of the entire aggregate is much slower than the time domain of this investigation. The rotational relaxation time of the complex can be estimated as $\tau_{rot} = (\eta V)/(k_B T)$, where η is solution viscosity, V is volume of the particle, T is temperature, and k_B is Boltzmann's constant. This estimate shows that the rotational relaxation will take place on a time scale of 2−10 ns, depending on assumed volume of the complex, which is in agreement with our data. As discussed in the last section, transient dipole moment measured in this experiment likely describes the whole aggregate (but not $TPPS_4$ monomers) and therefore constant r value suggests that aggregate structure does not change on this time scale.

TA and TAA Kinetics for Peptide−$TPPS_4$ Aggregates without Excitonic Coupling (pH 7.6). In an attempt to better characterize peptide−$TPPS_4$ complexes in neutral aqueous solutions, when J-aggregates are not formed, we again employed TA and TAA spectroscopy with excitation to the $TPPS_4$ Q_y band (S_1 state) at 520 nm. Intensity-dependent TA kinetics are shown in Figure 5 and fitting results are summarized in Table 3. As shown in the inset, ΔOD at $t = 0$ ps increases approximately linearly with excitation intensity, which shows that bleaching amplitude is proportional to concentration of excited $TPPS_4$. Fluorescence emission kinetics in Figure 2b have a nanosecond component with a lifetime similar to τ_3. Two faster components

TABLE 3: Transient Absorption Decay Parameters for Aggregates B3 (pH 7.6)[a]

excitation intensity, mJ cm^{-2}	ΔOD $\times$ 10^3 at t = 0 ps	amplitudes of decay components[b]		
		τ_1 = 5.1 ps	τ_2 = 93 ps	τ_3 > 3000 ps
1.5	12.6	33.4%	39.0%	27.6%
6.1	24.3	37.2%	39.9%	22.9%
10.2	56.8	45.8%	35.0%	19.2%
25.6	126.9	58.3%	26.6%	15.1%

[a] Pump and probe wavelengths 520 and 400 nm, respectively. Polarizations of pump and probe pulses were set at the magic angle. [b] Using the multiexponential fit $\Delta OD = A_1 \exp(-t/\tau_1) + A_2 \exp(-t/\tau_2) + A_3 \exp(-t/\tau_3)$, where ΔOD is transient absorption amplitude, A_i is fit component amplitude normalized as $A_i/(A_1 + A_2 + A_3) \times 100\%$, and τ_i is a lifetime.

τ_1 and τ_2 are also required to fit data in Figure 5. The amplitudes of components τ_1 and τ_2 increase with higher excitation intensity. Using arguments described earlier, τ_1 and τ_2 are attributed to singlet exciton annihilation. The fastest component τ_1 is attributed to annihilation when three excitations are created in one aggregate, while component τ_2 is due to annihilation when two excitations are present in one aggregate. The weaker coupling between the porphyrins at neutral pH leads to slower energy transfer time in the system; annihilation component τ_1 is 17 times slower at pH 7.6 than at pH 3.6 (0.3 vs 5.1 ps), while component τ_2 is 31 times slower (3 vs 93 ps).

We also investigated transient absorption anisotropy at pH 7.6. In contrast to the results in acidic solutions (Figure 4), we found that in neutral solutions the TA kinetics with collinear and perpendicular polarizations of pump and probe pulses were indistinguishable within signal-to-noise ratio for the experiment, and therefore anisotropy $r \approx 0$. The time resolution of our experiment was ~100 fs. It is unlikely that the energy transfer between weakly interacting $TPPS_4$ molecules could be faster than 100 fs, so it is unlikely that the negligible r value is caused by the very fast depolarization due to exciton migration. We evidently do not create absorption bleaching anisotropy in this experiment as described in the last section.

Energy Transfer in Peptide−$TPPS_4$ Aggregates and Aggregate Molecular Structure Considerations. Some estimates of the energy transfer time between porphyrins, $\tau_{hopping}$, could be obtained using models developed to analyze similar questions in photosynthetic antennas and self-assembled aggregates. A following simple relationship is based on a migration-limited annihilation model[24,25,31,32]

$$\tau_{annihilation} = \frac{N^2 - 1}{24}\tau_{hopping} \quad (2)$$

where N is the number of hopping sites (number of $TPPS_4$ molecules) and $\tau_{annihilation}$ is two-exciton annihilation time. For peptide−$TPPS_4$ aggregates studied here $N = 3$ and $\tau_{hopping} = 3\tau_{annihilation}$. When using the two-exciton annihilation component τ_2 from Tables 2 and 3, we obtain $\tau_{hopping} = 9$ ps at pH 3.6 and $\tau_{hopping} = 279$ ps at pH 7.6. Faster energy transfer time in acidic solutions could be attributed to (i) shorter distances between the monomers, (ii) a more favorable orientation of transition dipole moments, and/or (iii) better spectral overlap between emission and absorption spectra. The calculation based on absorption and fluorescence emission spectra in Figures 1 and 2 indicates that spectral overlap is approximately 9 times larger in acidic solutions. The energy transfer rate constants in these two environments differ by a factor of 31 times, thus orientation and/or distance effects must also be contributing to the changes in energy transfer rate constants by a factor of about three. When the peptide assumes an α-helical secondary structure at pH 7.6, the molecular geometry of the peptide backbone is more constrained than at pH 3.6, when peptide is in a random-coil conformation. This reduction in flexibility limits the possible orientations of the lysine side chains thereby restricting the orientation of bound $TPPS_4$ monomers, likely preventing them from adopting a conformation suitable for J-aggregate formation. This lack of spatial flexibility may also result in an increased distance between $TPPS_4$ monomers in the peptide-bound form at neutral pH. That is, formation of peptide α-helical secondary structure precludes formation of $TPPS_4$ J-aggregates when the (i, i+1, i+4) PBR is used to bind three $TPPS_4$ sulfonate groups, and energy transfer rate constant is smaller at neutral pH.

Finally, we examine if TA anisotropy data can provide additional information about the aggregate structure and energy transfer in this system. The porphyrin Soret band is composed of several sub-bands arising from different orientations of transition dipole moments predominantly located within the plane of porphine macrocycle.[33] Therefore only weak linear dichroism has been observed in the Soret band region for porphyrin derivatives and weakly interacting porphyrin aggregates.[34,35] In our experiments, the probe wavelength was in the Soret band region, where the energies of the transition dipole moments in the x and y direction (Scheme 1) are almost degenerate,[36] and anisotropy values due to $TPPS_4$ monomers are expected to be low. This is likely to be the case for aggregates **B3** when the excitation of the Q_y band at 520 nm does not create absorption bleaching anisotropy at 400 nm. In acidic solutions, the excitonically coupled aggregate acquires a large linear dipole moment, which integrates dipole moments of the individual molecules.[37] For $TPPS_4$ J-aggregates without peptides or other supporting scaffolds, the transition dipole moment of the 490 nm band is aligned along the longest axis of the aggregate.[18] Because aggregates studied here have absorption, fluorescence emission, resonance light scattering, and CD spectra that are similar to those of larger $TPPS_4$ aggregates,[15] the orientation of the 490 nm transition dipole moment of an aggregate is likely to be the same. Thus, for sample **B2** at pH 3.6, anisotropy has maximal value $r \approx 0.4$ due to the large transition dipole moment of J-aggregate. As the structure of the peptide−$TPPS_4$ J-aggregate does not change on the <1 ns time scale, anisotropy value remains constant (Figure 4).

In conclusion, for a system that could be described by a large aggregate dipole moment with smaller monomer dipole moments, a study of singlet exciton annihilation provides detailed information about the energy transfer within the aggregate (i.e., between the individual $TPPS_4$ molecules within the aggregate). TA anisotropy kinetics does not directly reflect energy transfer within one aggregate but provides supporting information about the absence of energy transfer between aggregates and suggests that excitonic coupling (that is, structure and spectra) of the system does not change on the time scale of TAA study.

In summary, we observed different porphyrin−porphyrin energy transfer rates in self-assembled peptide−$TPPS_4$ aggregates that have partially α-helical or random peptide secondary structure. Energy transfer time between porphyrins increases from 9 to 279 ps, or more than 30 times, when peptide secondary structure changes from random to α-helical. This change is due to electrostatic interactions that very strongly depend on solution acidity and control not only aggregate structure but also energy transfer dynamics. Such sensitivity of energy transfer on aggregate structure could be utilized in designing self-as-

sembling artificial photosynthetic complexes for light-harvesting applications or fluorescent sensors in which emission properties are dependent on peptide backbone conformation (which, in turn, depend on the acidity of the environment).

One long-term goal of these studies is to design peptide scaffolds that promote self-assembly of excitonically coupled porphyrins. The results presented here and in previous work[15] clearly show that while strong binding affinity is beneficial, tight binding is not sufficient for self-assembly. The ability to form J-aggregates requires conformational flexibility in the peptide backbone to achieve proper orientation of porphyrin monomers. Although the lysine side chain is long and flexible, the α-helical conformation may be too rigid to allow the lysines to optimally interact with multiple $TPPS_4$ monomers. Future designs can be aided by this knowledge through incorporation of more flexible cationic groups in the PBR or through the use of helix disfavoring residues.

Acknowledgment. Acknowledgment is made to the Donors of the American Chemical Society Petroleum Research Fund for partial support of this research. This work was partly supported by the Lithuanian Science Council Student Research Fellowship Award to J.K.

References and Notes

(1) Ke, B. *Photosynthesis: Photobiochemistry and photobiophysics*; Kluwer Academic Publishers: Dordrecht, 2001.

(2) Gust, D.; Moore, T. A.; Moore, A. L. *Acc. Chem. Res.* **2000**, *34*, 40–48.

(3) Discher, B. M.; Noy, D.; Strzalka, J.; Ye, S.; Moser, C. C.; Lear, J. D.; Blasie, J. K.; Dutton, P. L. *Biochemistry* **2005**, *44*, 12329–12343.

(4) Noy, D.; Discher, B. M.; Rubtsov, I. V.; Hochstrasser, R. M.; Dutton, P. L. *Biochemistry* **2005**, *44*, 12344–12354.

(5) Antonkine, M. L.; Koay, M. S.; Epel, B.; Breitenstein, C.; Gopta, O.; Gärtner, W.; Bill, E.; Lubitz, W. *Biochim. Biophys. Acta, Bioenerg.* **2009**, *1787*, 995–1008.

(6) Fry, H. C.; Lehmann, A.; Saven, J. G.; DeGrado, W. F.; Therien, M. J. *J. Am. Chem. Soc.* **2010**, *132*, 3997–4005.

(7) Bender, G. M.; Lehmann, A.; Zou, H.; Cheng, H.; Fry, H. C.; Engel, D.; Therien, M. J.; Blasie, J. K.; Roder, H.; Saven, J. G.; DeGrado, W. F. *J. Am. Chem. Soc.* **2007**, *129*, 10732–10740.

(8) McAllister, K. A.; Zou, H.; Cochran, F. V.; Bender, G. M.; Senes, A.; Fry, H. C.; Nanda, V.; Keenan, P. A.; Lear, J. D.; Saven, J. G.; Therien, M. J.; Blasie, J. K.; DeGrado, W. F. *J. Am. Chem. Soc.* **2008**, *130*, 11921–11927.

(9) Finikova, O. S.; Troxler, T.; Senes, A.; DeGrado, W. F.; Hochstrasser, R. M.; Vinogradov, S. A. *J. Phys. Chem. A* **2007**, *111*, 6977–6990.

(10) Cochran, F. V.; Wu, S. P.; Wang, W.; Nanda, V.; Saven, J. G.; Therien, M. J.; DeGrado, W. F. *J. Am. Chem. Soc.* **2005**, *127*, 1346–1347.

(11) Urbanová, M.; Setnička, V.; Král, V.; Volka, K. *Pept. Sci.* **2001**, *60*, 307–316.

(12) Kokona, B.; Kim, A. M.; Roden, R. C.; Daniels, J. P.; Pepe-Mooney, B. J.; Kovaric, B. C.; de Paula, J. C.; Johnson, K. A.; Fairman, R. *Biomacromolecules* **2009**, *10*, 1454–1459.

(13) Kovaric, B. C.; Kokona, B.; Schwab, A. D.; Twomey, M. A.; de Paula, J. C.; Fairman, R. *J. Am. Chem. Soc.* **2006**, *128*, 4166–4167.

(14) PyMOL software was used to illustrate peptide−porphyrin binding. DeLano, W. L. *The PyMOL Molecular Graphics System*; DeLano Scientific LLC: Palo Alto, CA, 2008.

(15) Kuciauskas, D.; Caputo, G. A. *J. Phys. Chem. B* **2009**, *113*, 14439–14447.

(16) Matsuzaki, K. *Biochim. Biophys. Acta, Biomembr.* **1999**, *1462*, 1–10.

(17) Shai, Y. *Biochim. Biophys. Acta, Biomembr.* **1999**, *1462*, 55–70.

(18) Ohno, O.; Kaizu, Y.; Kobayashi, H. *J. Chem. Phys.* **1993**, *99*, 4128.

(19) Hosomizu, K.; Oodoi, M.; Umeyama, T.; Matano, Y.; Yoshida, K.; Isoda, S.; Isosomppi, M.; Tkachenko, N. V.; Lemmetyinen, H.; Imahori, H. *J. Phys. Chem. B* **2008**, *112*, 16517–16524.

(20) Maiti, N. C.; Mazumdar, S.; Periasamy, N. *J. Phys. Chem. B* **1998**, *102*, 1528–1538.

(21) Gulbinas, V.; Karpicz, R.; Augulis, R.; Rotomskis, R. *Chem. Phys.* **2007**, *332*, 255–261.

(22) Holt, N. E.; Zigmantas, D.; Valkunas, L.; Li, X.-P.; Niyogi, K. K.; Fleming, G. R. *Science* **2005**, *307*, 433–436.

(23) Andrade, S. M.; Costa, S. M. B. *Biophys. J.* **2002**, *82*, 1607–1619.

(24) Hwang, I.-W.; Yoon, Z. S.; Kim, J.; Kamada, T.; Ahn, T. K.; Aratani, N.; Osuka, A.; Kim, D. *J. Photochem. Photobiol., A* **2006**, *178*, 130–139.

(25) Hwang, I.-W.; Kamada, T.; Ahn, T. K.; Ko, D. M.; Nakamura, T.; Tsuda, A.; Osuka, A.; Kim, D. *J. Am. Chem. Soc.* **2004**, *126*, 16187–16198.

(26) Sundstrom, V.; Gillbro, T.; Gadonas, R. A.; Piskarskas, A. *J. Chem. Phys.* **1988**, *89*, 2754–2762.

(27) Henk, F.; Jasper, K.; Douwe, A. W. *J. Chem. Phys.* **1993**, *98*, 6564–6566.

(28) *J-Aggregates*; Kobayashi, T., Ed.; World Scientific Publishing Company: River Edge, NJ, 1996.

(29) Perutz, M. F.; Wilkinson, A. J.; Paoli, M.; Dodson, G. G. *Annu. Rev. Biophys. Biomol. Struct.* **1998**, *27*, 1–34.

(30) Lakowicz, J. R. *Principles of Fluorescence spectroscopy*, 2nd ed.; Springer: New York, 1999.

(31) Bradforth, S. E.; Jimenez, R.; van Mourik, F.; van Grondelle, R.; Fleming, G. R. *J. Phys. Chem.* **1995**, *99*, 16179–16191.

(32) Kim, P.; Lim, J. M.; Yoon, M.-C.; Aimi, J.; Aida, T.; Tsuda, A.; Kim, D. *J. Phys. Chem. B* **2010**, *114*, 9157–9164.

(33) Sundholm, D. *Phys. Chem. Chem. Phys.* **2003**, *5*, 4265–4271.

(34) Ruban, A. V.; Calkoen, F.; Kwa, S. L. S.; van Grondelle, R.; Horton, P.; Dekker, J. P. *Biochim. Biophys. Acta, Bioenerg.* **1997**, *1321*, 61–70.

(35) Fuchs, H.; Zimmermann, J.; Röder, B. *Opt. Commun.* **2003**, *220*, 119–127.

(36) Gouterman, M. *In The Porphyrins*; Dolphin, D., Ed.; Academic Press: New York, 1978; Vol. 3, pp 1−166.

(37) Vlaming, S. M.; Augulis, R.; Stuart, M. C. A.; Knoester, J.; van Loosdrecht, P. H. M. *J. Phys. Chem. B* **2009**, *113*, 2273–2283.

JP108685N